EXPLOITING RECONFIGURABLE ANTENNAS IN COMMUNICATION SYSTEMS WITH DELAY-SENSITIVE APPLICATIONS

A Thesis

by

EMAN MAHMOUD HAMMAD

Submitted to the Office of Graduate Studies of
Texas A&M University
in partial fulfillment of the requirements for the degree of

MASTER OF SCIENCE

December 2011

Major Subject: Electrical Engineering

EXPLOITING RECONFIGURABLE ANTENNAS IN COMMUNICATION SYSTEMS WITH DELAY-SENSITIVE APPLICATIONS

A Thesis

by

EMAN MAHMOUD HAMMAD

Submitted to the Office of Graduate Studies of
Texas A&M University
in partial fulfillment of the requirements for the degree of

MASTER OF SCIENCE

Approved by:

Chair of Committee,	Jean-Francois Chamberland
Committee Members,	Henry D. Pfister
	Jim Xiuquan Ji
	Mahmoud M. El-Halwagi
Head of Department,	Costas N. Georghiades

December 2011

Major Subject: Electrical Engineering

ABSTRACT

Exploiting Reconfigurable Antennas in Communication Systems
with Delay-Sensitive Applications. (December 2011)
Eman Mahmoud Hammad, B.S., University of Jordan
Chair of Advisory Committee: Jean-Francois Chamberland

Wireless communication systems continue to face the challenge of time varying quality of the underlying communication channel. When a slow fading channel goes into a deep fade, the corresponding communication system might face successive decoding failures at the destination, and for delay-sensitive communication systems, this amounts to delays that are not desired. In such situations, it becomes a priority to get out of the deep fades. Many techniques and approaches are already available in the literature to counteract fading effects. This work is motivated by recent advances in fast reconfigurable antennas, which provide new means to change the statistical profile of fading channels, and hence reduce the probability of prolonged fades. Fast reconfigurable antennas are poised to improve overall performance, especially for delay-sensitive traffic in slow-fading environments. This potential enhanced performance motivates this study of the queueing behavior of point-to-point communication systems with reconfigurable antennas. We focus on finite-state channels with memory, and we analyze the queueing behavior of the wireless communication system over erasure channels, for a traditional system versus a reconfigurable antenna implementation. We provide numerical results for situations where using reconfigurable antennas yield substantial performance gains in terms of throughput, delay and buffer overflow.

DEDICATION

To the soul of my extraordinary mom “Laila J. Sanad”, family, Abdul, and my sweet angels Laila, Malak and “Salam Noor”.

ACKNOWLEDGMENTS

I am grateful and thankful to God's infinite blessings and mercy, for granting me the opportunity to be a graduate student in this department, and to experience a totally different learning experience for which I would always be appreciative.

I wish to express my sincere and deep gratitude to my advisor, Jean-Francois Chamberland, for his continuous support, guidance, trust, patience and encouragement. I cannot help but be in debt to him for his precious insight and discussions.

I would like to thank my colleagues at the Department of Electrical and Computer Engineering. Particularly, the Wireless Communication Lab group for the valuable experience and technical insight and discussions through the group meetings. I especially want to thank Santhosh Kumar for his input and help during this work. In addition, I want to extend my gratitude to my professors: Henry Pfister, Jim Ji and Mahmoud El-Halwagi, for being on my committee and for their support on different levels. I am very thankful to all my professors at Texas A&M who made my learning experience here an extraordinary one.

A special thanks goes to my friends here in the United States for their sincere good wishes and support during the past years.

In the end, I wish to thank my husband Abdallah Farraj, for his continuous encouragement, support on all frontiers, and for always believing in me.

TABLE OF CONTENTS

LIST OF FIGURES

FIGURE Page

CHAPTER I

INTRODUCTION

Wireless communication technologies and mobile applications are constantly gaining in popularity. As a consequence, the evolving demands and expectations of mobile users are reaching challenging levels in terms of data rate and delay requirements. This puts increasing pressure on an already strained cellular infrastructure, with its limited spectral bandwidth and costly hardware upgrades. Delay-sensitive services such as voice over internet protocol (VoIP), video conferencing, mobile gaming; and advanced video-aided applications like telepresence, video surveillance, e-healthcare can impose strict delivery requirements on the associated traffic flow. These restrictions must be accounted for while designing the components of the underlying communication system. A major challenge for digital communication over wireless channels is the constantly changing quality of physical connections. When a slow fading channel deteriorates and slips into a deep fade, the corresponding communication system must confront the eminent prospects of successive decoding failures and undue delay. In such a scenario, it becomes crucial to rapidly get the communication link out of the deep fade.

Several techniques have been proposed in the past to overcome or ease the adverse effects of fading [1, 2]. These approaches include time diversity and interleaving, space diversity and space-time codes, cooperation and multitone signaling.

Space diversity can be leveraged at the transmitter and receiver to counteract fading by averaging the signal over multiple independent paths, particularly in multiple-input multiple-output (MIMO) systems [3, 4]. Adaptive coding-modulation

---

The journal model is *IEEE Transactions on Automatic Control.*

techniques that respond to the status of the wireless channel have also been proposed [5, 6]. We emphasize that there is a natural tension between diversity and throughput. This phenomenon is typically studied in an asymptotic setting, and it is commonly known as the diversity-multiplexing tradeoff.

Diversity approaches can lead to substantial gains in performance. A similar fundamental tradeoff between multiplexing gain, diversity and delay has been identified and studied in several contexts. Still, many contributions on the benefits of diversity overlook the queueing aspect of the problem, which is especially important in the context of delay-sensitive applications.

In this thesis, we consider reconfigurable antennas as a possibly new strategy to counteract the effects of fading on wireless communication. We are especially interested in delay-sensitive applications. From an abstract point of view, our approach takes advantage of channel diversity at the physical layer by increasing the number of virtual channel realizations from the source to the destination. This added flexibility comes at a price: the reconfiguration process takes time and can invalidate the transmission of symbols for a pre-determined time interval.

Reconfigurable antenna technologies are collectively emerging as a viable option for smart phones, mobile hotspots, and portable computers [7, 8, 9, 10, 11]. This class of antennas can be employed in a number of ways to enhance the connectivity profile and robustness of wireless communication channels. These antennas create new and promising opportunities for the engineering of superior communication schemes. Such antennas are designed to intentionally and reversibly alter the character of their performance-governing electromagnetic fields. As a result, they are able to modify the directional and polarization properties of their radiation patterns and thereby change the spatiotemporal characteristics of the communication channels they induce.

Beyond the basic properties of reconfigurable antennas, it is interesting to note

that the manipulations of radiation patterns can be automated through rapid feedback and triggered by events such as deep fades and successive decoding failures [12, 13, 14, 15]. This enables the implementation of closed-loop systems with the cognitive ability to seamlessly adapt to evolving electromagnetic environments and interference conditions. The capacity to provide these features in (near) real time is primarily determined by the speed and complexity of the reconfiguration mechanisms used to facilitate electromagnetic agility within the reconfigurable antenna structures. This points to the potential benefits of a configuration change and, also, to the downtime associated with each transformation event.

Although reconfigurable antennas have been and continue to be the subject of concerted research efforts in the antennas and propagation community, a detailed analysis of their repercussions on the foundations of wireless communications is still lacking. Key to the widespread adoption of such technologies, aside from small-scale implementations, is provable gains in terms of capacity, delay-throughput profile and network connectivity [16, 17]. Herein, we seeks to better understand the impact of adaptive antennas on the queued performance of communication systems at a fundamental level.

Fast reconfigurable antennas can be employed to establish ancillary virtual links between two devices. As the quality of the current channel degrades, it may become advantageous to transition to an alternate antenna state and, consequently, to another channel realization. This added flexibility at the physical layer is likely to boost the perceived performance of delay-sensitive applications over channels with memory. Indeed, several studies document the fact that channel variations are particularly detrimental to delay-constrained communications [18, 5, 19, 6]. Channel memory further exacerbates this situation, as it increases the propensity for prolonged deep fades [20, 21]. Having the capability to jump to a different virtual channel seems an

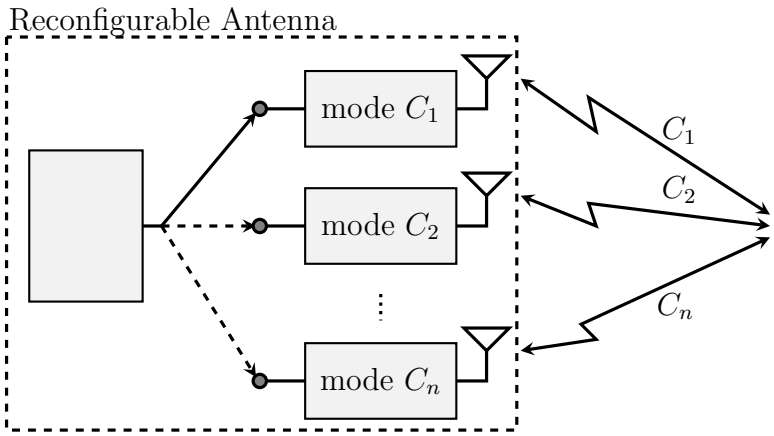

Fig. 1. A conceptual diagram of a reconfigurable antenna showing the switching and virtual channels.

attractive option in these circumstances. Fig. 1 shows a diagram that illustrates the concept of virtual channels induced by a reconfigurable antenna.

To uncover the benefits of reconfigurable antennas in the context of delay-sensitive communications, we leverage several results that have appeared in the literature. First, we adopt a class of models for channels with memory similar to the finite-state channel model proposed by Gilbert and Elliott [22, 23]. The delay-sensitive aspect of the problem is captured through a queueing formulation whose solution is obtained, partly, by applying techniques originally developed by Neuts [24, 25, 26]. The conceptual bridge between the physical layer and the queued system is provided by error-correcting codes and the availability of feedback. The framework to be presented later parallels some of the previous work performed by Parag et al. [21]. The incorporation of reconfigurable antennas into the problem setting and the insights obtained through our analysis are novel. This sheds new light on the potential ben-

efits of adaptive antenna systems and their application to delay-sensitive traffic over wireless channels.

A. Problem Statement

We consider a point-to-point wireless communication system that support delay-sensitive applications; these applications are subject to stringent service constraints. The communication channel at the physical layer is modeled as a finite-state channel with memory. We assume that the transmitter possesses partial channel-state information and that it can be equipped with reconfigurable antennas. Moreover, we postulate that the encoder utilizes a random coding scheme. Furthermore, packet receptions are acknowledged through reliable feedback. This communication link is poised to support delay-sensitive applications, with a soft queueing constraint. We wish to quantify and analyze the performance gains associated with the reconfigurable system compared to the traditional implementation.

B. Thesis Structure

The remainder of this document is organized as follows. Chapter II provides a survey of important results and challenges associated with delay-sensitive communication, with special attention to analysis techniques and available tools. These tools will be used to build, study and ultimately solve our proposed research problem. The system components, along with a mathematical abstraction for reconfigurable antennas, are described in Chapter III. Two modes of operation are considered, a classical system with a static antenna structure and an adaptive implementation with the ability to reconfigure its RF front-end. The operation of these two competing alternatives is characterized in Chapter IV, where we examine their respective queueing behaviors.

This gives rise to several performance criteria including throughput, mean waiting time and the probability of the queue exceeding a certain threshold. Pertinent numerical examples are provided in Chapter V, followed by concluding remarks.

CHAPTER II

BACKGROUND

The time-variations in channel quality associated with wireless environments form a major challenge for mobile devices that seek to establish reliable, rapid connections. These fluctuations are intrinsic to wireless communications and are attributable to the movement of mobile devices as well as dynamic changes in their surroundings. In contrast to attenuation, which can be accurately estimated and controlled, fading is particularly detrimental to delay-sensitive applications. Indeed, a fast fluctuation profile can result in a significant probability that a communication channel experiences a deep fade.

A. Fading Channels

From a physical point of view, fading is caused by the constructive or destructive superposition of multiple copies of a same signal that travels through various paths. This process depends heavily on environmental conditions and can affect the received signal strength as well as the phase of the signal [1]. Furthermore, when a mobile device is in motion, there can be a shift in the central frequency of the waveform, as observed at the destination; this condition is known as the doppler effect. We review below a number of definitions pertinent to our future discussion.

- **Multipath:** This term refers to the arrival of multiple copies of a transmitted signal at the receiver displaced with respect to one another in time and spatial orientation. This phenomenon is a consequence of the presence of reflecting objects and scatterers in wireless environments. The misalignment in phase and amplitude of the different paths causes fluctuations in the overall strength

of the received signal, which leads to fading [1].

- **Coherence Bandwidth:** When the spectral bandwidth of the transmitted signal is large, disjoint intervals of the spectrum may experience unequal fade levels. In this case, the resulting channel is said to feature frequency-selective fading. The range of frequencies over which the channel can be considered approximately flat is called the coherence bandwidth, B_c [27].

- **Doppler Shift:** This is the apparent shift in frequency of a signal due to the transmitter and/or receiver moving. It is typically expressed by the relation $f_d = \frac{v}{\lambda}\cos\theta$, where v denotes the receiver velocity toward the transmitter, λ is the carrier wavelength, and θ is the angle of arrival of the received signal relative to the direction of motion [27].

- **Coherence Time:** This quantity captures how fast a channel is changing over time. Mathematically, the coherence time, T_c, is a statistical measure of the duration over which the channel impulse response remains essentially invariant. The amplitude of the received signal within this time interval is strongly correlated. Generally speaking, the coherence time is inversely proportional to the Doppler spread, $T_c \propto \frac{1}{f_m}$ [1].

B. Finite-State Markov Modeling of Fading Channels

Finite-state communication channels with memory have been the subject of studies for several decades, and can be traced in the work by Shannon in 1957[28].

Many extensions have been considered since their initial introduction. Notable developments to finite-state channels include seminal contributions by Gilbert and Elliott. Gilbert presented a two-state Markov channel model in which the input-

output relationship depends on the current state of the channel [22]. Elliott later expanded this model by incorporating a larger class of error profiles; this enhanced model was originally employed to analyze the performance of error-correcting codes over bursty channels [23]. The combined efforts of Gilbert and Elliott led to the famed Gilbert-Elliott channel, shown in Fig. 2.

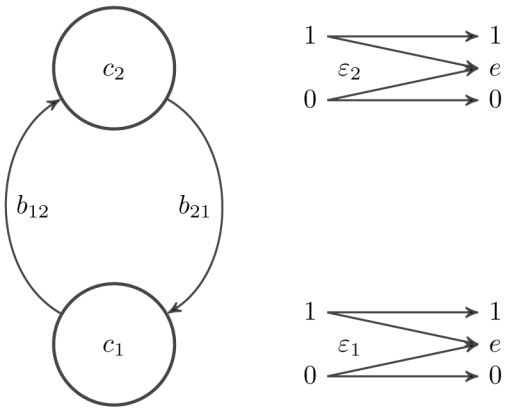

Fig. 2. A finite-state channel with memory. A two states model known as the Gilbert-Elliott channel.

In its abstract form, the channel has two states, a good state G and a bad state B. The probability that a bit is received faithfully at the destination depends on the state of the channel, and can be expressed as a conditional crossover probability. The instantaneous error probability is a measure of channel quality. Furthermore, the evolution of the channel over time forms a Markov chain. The transition probabilities between the states determine the stationary distribution of the chain and also capture channel memory.

The Gilbert-Elliott channel model can be modified to include more states. The extra degrees of freedom associated with additional states result in a more intricate abstraction and can, in certain circumstances, improve model accuracy. Collectively,

these channels are termed finite-state channels with memory. This class of channel models has successfully been applied to wireless communication links in the past [29, 18, 30].

An important quality behind finite-state channels with memory is that they often yield mathematically tractable formulations and accurate results. Indeed, the vast literature on Markov chains can be applied to problems in wireless communication when an appropriate channel structure is selected. In many situations, Markov models lead to insightful analytical solutions rather than numerical results obtained through simulations; this is exemplified below.

The work of Wang and Moayeri provides an explicit relation between a statistical fading description, Clark's model for Rayleigh fading, and a finite-state channel with memory [29]. The methodology described in their paper first partitions the received signal-to-noise ratio (SNR) into disjoint intervals, every interval representing a distinct channel state.

The marginal probability of error, conditioned on the prescribed interval, is then used as the designated crossover probability for the Markov state. This mapping can be refined by simply adding states to the Markov model. Transition probabilities of the Markov model are then estimated based on up-crossing rates. Modifications to this approach are possible [31]. For instance, in certain circumstances, only adjacent state transition are admitted. This may depend on the modulation scheme employed, the power budget and the spectral profile of a wireless environment.

The memory order of a Markov model may refer to how many previous states affect the selection of the next state. In a first-order Markov model, the selection of state C_i given C_{i-1} is independent of anterior channel history. First-order finite-state channels with memory are found to be accurate for reasonably slow fading, with a normalized fading rate $\overline{f}_d T_s \leq 0.01$, where $\overline{f}_d$ is the maximum Doppler shift and

T_s is the symbol period. This conclusion is rather intuitive since, for a slow fading channel, knowledge of preceding states would offer little additional information. In such scenarios, the most recent state captures the essence of time dependency. In the intermediate fading regime, higher-order Markov models can lead to better accuracy. Finite-state channels with memory are used in several applications. They form a powerful abstraction for modeling communication channel with error bursts. They can be used to assess how correlation over time affects the capacity of communication channels. Furthermore, they are suitable to analyze the queueing performance of communication links. Finally, they are amenable to the simulation of complex systems through Markov Chain Monte Carlo methods.

C. Matrix Geometric Method

The matrix geometric method, is a technique originally developed by Neuts [25] to derive the stationary distribution of queued systems with repetitive structures. For instance, this technique can be applied to queueing processes with phase-type service.

In such situations, the state space of the whole system can be divided into levels [25, 26]. The entries of the corresponding transition probability matrix can be grouped into finite submatrices and, based on this structure, the evolution of the queued system displays an elegant symmetry.

Since the matrix geometric method is inherently a numerical procedure, it is frequently used to find the desired distribution when a closed-form solution is hard to obtain.

The matrix geometric method can also be applied to study certain communication systems with random arrivals and changing channel conditions. In this latter scenario, the system state may reduce to a discrete-time quasi-birth-death process.

The states of a quasi-birth-death process can typically be arranged as

$$S = \{(i, q)|0 \leq i, 0 \leq q \leq m\},$$

where i identifies the current jump rates of the process, and q represents the number of elements in the system. With a proper ordering of the states, one can recognize a block structure in the transition probability matrix of the aggregate system. The resulting submatrices specify the transition probabilities among levels and they can be further divided into two groups: an irregular set subject to boundary conditions and repetitive blocks with a regular structure.

1. Quasi-Birth-Death Process

We label boundary blocks using $\mathbf{C}$ and we employ $\mathbf{A}$ to represent regular components. Suppose that the Markov system is stable and assume that transitions are only possible among adjacent states. Furthermore, assume that transitions probabilities for non-zero levels possess a repetitive structure. Then, without loss of generality, the probability transition matrix of the discrete-time quasi-birth-death process can be written in block form as

$$\mathbf{T} = \begin{pmatrix} \mathbf{C}_1 & \mathbf{C}_0 & \mathbf{0} & \mathbf{0} & \cdots \\ \mathbf{A}_2 & \mathbf{A}_1 & \mathbf{A}_0 & \mathbf{0} & \cdots \\ \mathbf{0} & \mathbf{A}_2 & \mathbf{A}_1 & \mathbf{A}_0 & \cdots \\ \mathbf{0} & \mathbf{0} & \mathbf{A}_0 & \mathbf{A}_2 & \cdots \\ \vdots & \vdots & \vdots & \vdots & \ddots \end{pmatrix}. \tag{2.1}$$

The states $\{(1, q), (2, q), \ldots, (n, q)\}$ are known as the qth level of the chain. Let

$$\pi_q = \begin{bmatrix} \pi(1, q) & \pi(2, q) & \cdots & \pi(n, q) \end{bmatrix}$$

be the stationary distribution associated with the qth level and, similarly, let

$$\pi = \begin{bmatrix} \pi_1 & \pi_2 & \cdots \end{bmatrix}$$

denote the invariant distribution of the entire system. We know from the Chapman-Kolmogorov equations that $\pi\mathbf{T} = \pi$. One possible approach to calculate the stationary distribution π numerically is to use the matrix geometric method.

Theorem C.1 (Neuts [25]) *Consider a positive recurrent, irreducible Markov chain on a countable state space with transition probabilities given by* (2.1)*. Let matrix* $\mathbf{U}$ *be defined such that the* (c, d) *entry is the probability that, starting from state* $(1, c)$*, the Markov chain first re-enters level one by visiting* $(1, d)$ *and does so without visiting any state at level zero. The substochastic matrix* $\mathbf{U}$ *may be computed as the limit, starting from* $\mathbf{U}_1 = \mathbf{A}_1$*, of the sequence defined by*

$$\mathbf{U}_{j+1} = \mathbf{A}_1 + \mathbf{A}_0 \left(\mathbf{I} - \mathbf{U}_j\right)^{-1} \mathbf{A}_2. \tag{2.2}$$

Let matrix $\tilde{\mathbf{T}}$ *be given by*

$$\tilde{\mathbf{T}} = \begin{bmatrix} \mathbf{C}_1 & \mathbf{C}_0 \\ \mathbf{A}_2 & \mathbf{A}_1 + \mathbf{R}\mathbf{A}_2 \end{bmatrix} \tag{2.3}$$

where $\mathbf{R} = \mathbf{A}_0 \left(\mathbf{I} - \mathbf{U}\right)^{-1}$*. Then,* $\tilde{\mathbf{T}}$ *is a stochastic matrix associated with a finite and irreducible Markov chain. If we denote the invariant distribution associated with* $\tilde{\mathbf{T}}$ *by* $[\tilde{\pi}_0\ \tilde{\pi}_1]$*, then the stationary distribution associated with* $\mathbf{T}$ *can be expressed as*

$$\begin{aligned} \pi_0 &= \frac{\tilde{\pi}_0}{(\tilde{\pi}_0 + \tilde{\pi}_1(\mathbf{I} - \mathbf{R})^{-1})\,\mathbf{1}} \\ \pi_q &= \frac{\tilde{\pi}_1 \mathbf{R}^{q-1}}{(\tilde{\pi}_0 + \tilde{\pi}_1(\mathbf{I} - \mathbf{R})^{-1})\,\mathbf{1}} \end{aligned} \tag{2.4}$$

where $q \geq 1$*.*

We emphasize that, in finding a solution to the matrix equation

$$\pi_q \mathbf{A}_1 = \pi_{q-1} \mathbf{A}_0 + \pi_q \mathbf{A}_1 + \pi_{q+1} \mathbf{A}_2,$$

the form of the embedded Markov structure and, specifically, its block partitioning are far more important than the precise values of each submatrix. Key to our eventual analysis is to reduce the queueing problem we wish to study to the discrete-time, quasi-birth-death structure shown above.

CHAPTER III

SYSTEM MODEL

The overall system model that we use consists of a transmit buffer, an arrival process and a departure process, error correcting codes, and a physical channel model. We assume perfect channel state information at the source and, also, the availability of instantaneous feedback from destination to the transmitter. For the sake of simplicity, we focus on the information flow from the source to the destination. A similar analysis can be applied to the reverse link, if needed. To obtain pertinent measures for delay-sensitive communications, we study system performance using a queueing formulation. The queue state is governed by both arrivals and departures. Moreover, the evolution of the queue is modeled as a discrete-time stochastic process, which is synchronized with codeword transmissions. In particular, we assume that during each codeword cycle, a data packet arrives at the source with probability γ, independently of other time instances. In our model, the number of information bits per data packet, denoted by L, is random and possesses a geometric distribution with parameter ρ. Below, we describe the service models for both a system utilizing a reconfigurable antenna and a traditional implementation.

A. Traditional Implementation

We refer to a system that employs a static antenna as a traditional implementation. Our channel model for a wireless communication system with a fixed antenna is based on several possible modes of operation, which we denote by $\mathcal{C} = \{c_1, \ldots, c_k\}$. The evolution of the channel over time forms a homogeneous Markov process, with a probability transition matrix $\mathbf{B}$, which we write as

$$\mathbf{B} = \begin{bmatrix} b_{11} & b_{12} & \cdots & b_{1k} \\ b_{21} & b_{22} & \cdots & b_{2k} \\ \vdots & \vdots & \ddots & \vdots \\ b_{k1} & b_{k2} & \cdots & b_{kk} \end{bmatrix}. \tag{3.1}$$

Above, b_{ij} represents the probability that the Markov chain transitions from state i to state j in one time step. The quality of the channel, conditioned on a specific state, is expressed in terms of a bit erasure probability. When the channel is in state i, a symbol sent by the transmitter is erased with probability ε_i or, equivalently, the symbol is observed at the destination with probability $1 - \varepsilon_i$. The elements of $\mathcal{C}$ are indexed in such a way that $i < j$ implies $\varepsilon_i \geq \varepsilon_j$. In words, if $i < j$, then channel state c_j is more reliable than channel state c_i. When this finite-state channel can take only two possible values, it is known as a Gilbert-Elliott erasure channel [22, 23]. A graphical representation of the Gilbert-Elliott erasure channel is shown in Fig. 3.

The system we envision employs error-control coding to counteract the adverse effects of channel uncertainty. Arriving packets at the source are sliced into data segments, each containing K information bits. Data segments are then encoded and transmitted as codewords of fixed length N to the destination. As per our channel model, individual symbols may be received at the destination or erased depending on the realization of the finite-state channel. Decoding is executed on a per codeword basis, and is attempted on a regular interval. An important quantity in our impending analysis is the distribution of the number of erasures per codeword, conditioned on the state of the channel at the onset of the transmission. There exist various strategies to compute such distributions. One possible approach is to first find the distribution of the channel states and then compute the conditional distribution on the number of erasures [32]. Alternatively, we can employ matrix generating functions with with

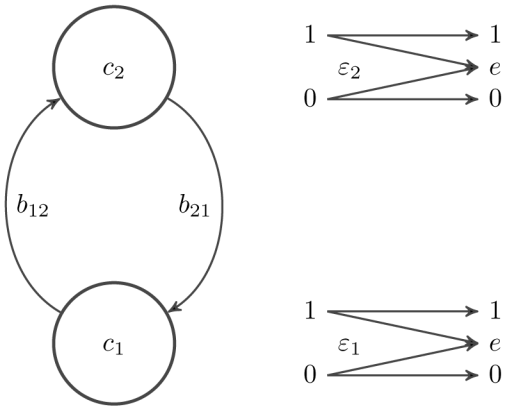

Fig. 3. A finite-state channel with memory is used to model the operation of a wireless link at the bit level. For illustrative purposes, the channel is depicted with only two states, a form known as the Gilbert-Elliott erasure channel.

polynomial entries to derive these quantities [33].

At this point, it suffices to point out that

$$\Pr(E = e, C_{N+1} = c_j | C_1 = c_i) \tag{3.2}$$

can be computed efficiently. Throughout, C_n represents the state of the channel at time n, and E denotes the number of erasures within a block.

We consider a system where every codebook is created using a random binary parity-check matrix $\mathbf{H}$ of size $(N - K) \times N$. The admissible codewords are the elements of the nullspace of $\mathbf{H}$. Decoding at the receiver is executed using a maximum likelihood decision rule. The probability of decoding failure, conditioned on e erasures, is given by

$$P_{\mathrm{f}}(N - K, e) = 1 - \prod_{i=0}^{e-1} \left(1 - 2^{i-(N-K)}\right) \tag{3.3}$$

where N is the code length and K designates the number of information bits per codeword [34]. Accounting for channel states, the conditional probability of decoding failure at the destination, which we represent by $P_{\mathrm{df}}(c_j; c_i)$, is given by

$$P_{\mathrm{df}}(c_j; c_i) = \sum_{e=0}^{N} P_{\mathrm{f}}(N-K, e) \Pr\left(E = e, C_{N+1} = c_j | C_1 = c_i\right).$$

Similarly, the conditional probability of decoding success, labeled $P_{\mathrm{ds}}(c_j; c_i)$, can be written as

$$P_{\mathrm{ds}}(c_j; c_i) = \sum_{e=0}^{N} (1 - P_{\mathrm{f}}(N-K, e)) \Pr\left(E = e, C_{N+1} = c_j | C_1 = c_i\right).$$

Hence, combining (3.2) and (3.3), we obtain the probability of transitioning to state c_j with or without decoding successfully, conditioned on the channel starting in state c_i. Collectively, these probabilities underly the evolution of the queued system.

To conform with our encoding scheme, a data packet of length L must be divided into $M = \lceil L/K \rceil$ segments, each of size K. The ending segment of a packet is zero-padded, if needed. Note that M is also a geometric random variable, albeit with parameter

$$\rho_r = \sum_{\ell=1}^{K} (1-\rho)^{\ell-1} \rho = 1 - (1-\rho)^K. \tag{3.4}$$

These segments are successively encoded into codewords of length N and sent over the finite-state channel. Upon successful decoding, the destination acknowledges reception of the information and the corresponding segment is discarded from the source buffer. On the other hand, when transmission fails, the source is notified. The leading data segment is then immediately re-encoded and transmitted once again over the wireless channel. This process continues until successful reception of the codeword.

The number of packets awaiting transmission is selected as the state of the queue.

This perspective reflects our inclination towards delay-sensitive communications. We stress that, in our framework, a packet departs from the queue if a codeword is decoded successfully at the destination and the received segment is the last parcel of information of the lead packet. When these two conditions are met, the lead packet is discarded from the queue.

We use Q_s to identify the state of the queue at discrete-time s. Although the stochastic process $\{Q_s\}$ does not possess the Markov property, it can be shown that the queue length and the channel state at the onset of a codeword cycle, jointly designated by $Y_s = (C_{sN+1}, Q_s)$, form a Markov chain [21].

The transition probabilities of this Markov chain can be calculated as follows. Suppose that the queue is non-empty, i.e., $Y_s = (c_i, q)$ where $q > 0$. Owing to our problem definition, the admissible values for Q_{s+1} are $\{q-1, q, q+1\}$. Several factors can affect the evolution of the queue over time: the arrival of a new packet, the successful decoding of a codeword and whether or not this latter codeword is the last segment of a data packet. The only scenario that leads to a decrease in the queue is having no arrival and one packet departure. Recall that a packet departure occurs when a codeword is successfully decoded and the corresponding segment is the last parcel of information of the lead data packet. This yields

$$\begin{aligned}\mu_{ij} &= \Pr(Y_{s+1} = (c_j, q-1) | Y_s = (c_i, q)) \\ &= (1-\gamma) P_{\mathrm{ds}}(c_j; c_i) \rho_r.\end{aligned}$$

For the queue length to remain at a same level, departures and arrivals must be balanced. In particular, there can be either no departure and no arrival, or one

departure and one arrival,

$$\begin{aligned}\kappa_{ij} &= \Pr(Y_{s+1} = (c_j, q) | Y_s = (c_i, q)) \\ &= (1-\gamma)\left(P_{\mathrm{df}}(c_j; c_i) + P_{\mathrm{ds}}(c_j; c_i)(1-\rho_r)\right) + \gamma P_{\mathrm{ds}}(c_j; c_i)\rho_r.\end{aligned}$$

Finally, the queue increases whenever a packet arrives and no departure occurs,

$$\begin{aligned}\lambda_{ij} &= \Pr(Y_{s+1} = (c_j, q+1) | Y_s = (c_i, q)) \\ &= \gamma\left(P_{\mathrm{df}}(c_j; c_i) + P_{\mathrm{ds}}(c_j; c_i)(1-\rho_r)\right).\end{aligned}$$

When the queue is empty, $Q_s = 0$, similar arguments apply, except that there can be no departures,

$$\begin{aligned}\kappa^0_{ij} &= \Pr(Y_{s+1} = (c_j, 0) | Y_s = (c_i, 0)) \\ &= (1-\gamma)\Pr(C_{(s+1)N+1} = c_j | C_{sN+1} = c_i) \\ \lambda^0_{ij} &= \Pr(Y_{s+1} = (c_j, 1) | Y_s = (c_i, 0)) \\ &= \gamma \Pr(C_{(s+1)N+1} = c_j | C_{sN+1} = c_i).\end{aligned}$$

Possible transitions for a non-empty queue at level q are depicted in Fig. 4. Again, for simplicity, the diagram assumes a two-state channel at the physical layer.

B. Reconfigurable Antenna Implementation

Although a series of carefully designed experiments in anechoic chambers have been reported previously in the literature on reconfigurable antenna systems [12, 8, 9], establishing accurate mathematical models for particular implementations can be a daunting task. Given that this is a preliminary investigation on the topic, we make simplifying assumptions that are somewhat favorable to RF-agile devices. The rational behind this reasoning is to gain insight without risking to prematurely discard a promising technology that may eventually lead to significant gains. We postulate that

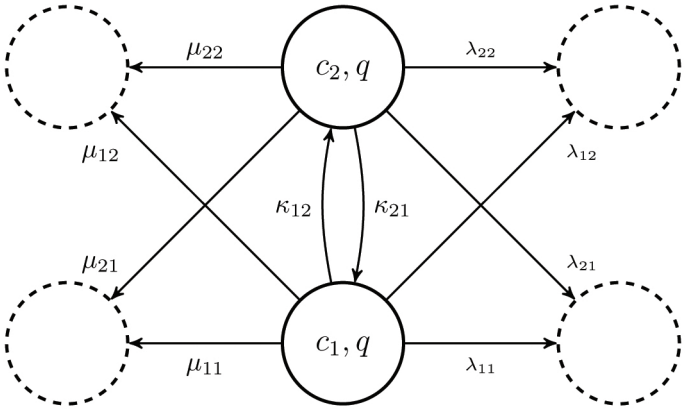

Fig. 4. Possible transitions with partial labeling for a queued system built upon a two-state channel model and operating using a fixed antenna configuration. Self-transitions are intentionally omitted.

reconfigurable antennas have a large number of possible configurations, and we assume that the wireless channels induced by these configurations are independent from one another. This is more likely to apply to situations where devices are embedded in rich scattering environments. A direct implication of these two hypotheses is that a wireless device equipped with a reconfigurable antenna can always elect to switch to a different virtual channel. Furthermore, once this transformation is accomplished, the probability that the wireless channel occupies a particular state becomes equal to the stationary probability of this same state.

A second aspect of reconfigurable antenna systems that warrants attention is the latency of the morphing process. The time necessary to execute an antenna reconfiguration depends heavily on the physics underlying the process. Applicable technologies relevant to our present investigation include electronic switches, micro-

electromechanical systems (MEMS) and microfluidic devices. Collectively, these miscellaneous techniques embody a range of options in terms of latency, efficiency and power consumption. They also offer fundamentally different mechanisms that can provide measurable tradeoffs between speed, power handling, linearity and overall complexity. Moreover, they each feature a compact form factor suitable for mobile devices. Based on the state-of-the-art for these mechanisms, it is reasonable to assume that reconfiguration latency is no greater than a typical codeword cycle (on the order of 4.615 ms). In our analysis, we assume that triggering an antenna reconfiguration event results in the loss of one codeword transmission opportunity. No segment can be decoded at this time and, as such, there cannot be a departure from the queue. This is the price to pay for the opportunity to access a fresh channel realization.

We consider static control policies for antenna handling that are based solely on channel state. Furthermore, we look at hierarchical structures: if c_j is deemed deficient enough to initiate a channel reconfiguration, then c_i will also trigger a reconfiguration whenever $i < j$. Implicit to such control policies is the presence of channel state information at the source. This construction, again, favors adaptive systems. More pragmatic schemes would have to employ state estimates or trigger a reconfiguration based on the number of successive failed decoding attempts. Still, our simplified framework is a logical starting point; if an adaptive system fails to produce significant gains when side information is available, there is no need to study more intricate formulations.

When the channel state is judged satisfactory, no reconfiguration takes place and the transition probabilities defined in Section A apply. On the other hand, when a system reconfiguration is initiated, the transition probabilities simply become

$$\tilde{\mu}_{ij} = \Pr(Y_{s+1} = (c_j, q-1) | Y_s = (c_i, q)) = 0$$

$$\tilde{\kappa}_{ij} = \Pr(Y_{s+1} = (c_j, q) | Y_s = (c_i, q)) = (1-\gamma) p_C(j)$$
$$\tilde{\lambda}_{ij} = \Pr(Y_{s+1} = (c_j, q+1) | Y_s = (c_i, q)) = \gamma p_C(j),$$

where $p_C(\cdot)$ is the marginal probability mass function on the channel states. We emphasize that the transition probabilities are completely determined by the latter probability mass function and the likeliness of a packet arrival, and they do not depend on the coding scheme. Also, we have

$$\tilde{\kappa}^0_{ij} = (1-\gamma) p_C(j)$$
$$\tilde{\lambda}^0_{ij} = \gamma p_C(j)$$

whenever a reconfiguration event is sparked from an empty queue.

Fig. 5 presents a level-transition diagram for a two-state channel where an antenna reconfiguration is prompted. This takes place every time the channel lies in the most inauspicious state at the onset of a codeword cycle.

It may be instructive to compare this graph with Fig. 4, whose labels embody the operation of a communication system with a static/fixed antenna structure.

This completes our description of the two queued systems, with and without reconfigurable antenna structures. In both cases, the state space for the discrete-time packetized system is $\mathcal{C} \times \mathbb{N}_0$. Each implementation will be stable provided that the average arrival rate is less than its expected service rate. When this is the case, the underlying Markov chain is positive recurrent and it admits a stationary distribution [35]. Next, we we examine stability conditions more closely and we provide means to compute invariant distributions. This is performed by linking the mathematical formulation of our problem to classical queueing results.

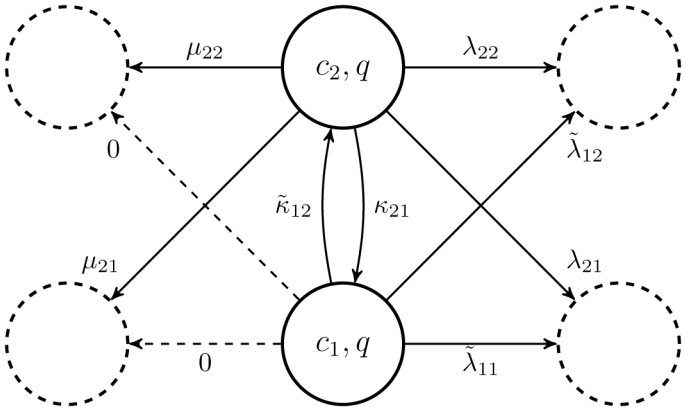

Fig. 5. In this diagram, the two-state antenna system evolves unaltered while in state (c_2, q); whereas an antenna reconfiguration is initiated whenever the system enters state (c_1, q). The reconfiguration process alters the transition probability of the system, as designated by the tildes.

CHAPTER IV

QUEUEING BEHAVIOR

As we have developed the system model for the traditional and the reconfigurable antenna implementations, we further analyze the system model with queueing tools to obtain performance measures that will facilitate a quantitative comparison between the two implementations, using numerical analysis, that would follow in chapter V

We first examine arrival and service rates. Recalling that a new data packet arrives at the source at time s with probability γ. The number of bits in every packet is a geometric random variable with parameter ρ, and hence, the number of segments contained in any packet is a geometric random variable with parameter ρ_r, as defined in (3.4). Thus, the expected arrival rate in segments per block is given by

$$\gamma \mathrm{E}\left[M\right] = \frac{\gamma}{\rho_r}.$$

The expected service rate depends on the communication scheme employed. In the traditional implementation with fixed antennas configuration, the evolution of the wireless channel is unaltered at the codeword boundaries. That is we realize the channel distribution for every N consequential usages of the channel and that is the codeword length, and this realization corresponds to the $\mathbf{B}^N$ matrix. Then we sum over the different states of the channel multiplied by the corresponding probability of successfully decoding at the destination P_{ds}. Thus we can express the throughput, which is the expected service rate, in segments per block as

$$\sum_{i \in \mathcal{C}} \sum_{j \in \mathcal{C}} P_{\mathrm{ds}}(c_j; c_i) p_C(c_i) \tag{4.1}$$

where $p_C(\cdot)$ is the stationary channel distribution associated with matrix

$$\mathbf{B}^N = \begin{bmatrix} b_{11}^{(N)} & b_{12}^{(N)} & \cdots & b_{1k}^{(N)} \\ b_{21}^{(N)} & b_{22}^{(N)} & \cdots & b_{2k}^{(N)} \\ \vdots & \vdots & \ddots & \vdots \\ b_{k1}^{(N)} & b_{k2}^{(N)} & \cdots & b_{kk}^{(N)} \end{bmatrix}. \tag{4.2}$$

We stress that, since $\mathbf{B}$ is assumed irreducible and aperiodic, its invariant distribution $p_C(\cdot)$ exists and is unique [36]. This distribution is also invariant for probability transition matrix $\mathbf{B}^N$, which justifies its use in (4.1).

Now we turn to the reconfigurable antennas case. First to obtain the probability transition matrix for the adaptive architecture with reconfigurable antennas. Let $\mathcal{C}^\dagger = \{\ell, \ldots, k\}$ represent the collection of channel states judged suitable for data transmission. Then, necessarily, the set $\mathcal{C} \setminus \mathcal{C}^\dagger$ contains all the channel states for which an antenna reconfiguration control command is issued. With this partitioning, we gather that the probability transition matrix for the channel state at the onset of a codeword cycle is

$$\tilde{\mathbf{B}}^{(N)} = \begin{bmatrix} p_C(1) & p_C(2) & \cdots & p_C(k) \\ \vdots & \vdots & \ddots & \vdots \\ p_C(1) & p_C(2) & \cdots & p_C(k) \\ b_{\ell 1}^{(N)} & b_{\ell 2}^{(N)} & \cdots & b_{\ell k}^{(N)} \\ \vdots & \vdots & \ddots & \vdots \\ b_{k1}^{(N)} & b_{k2}^{(N)} & \cdots & b_{kk}^{(N)} \end{bmatrix}. \tag{4.3}$$

We point out that matrix entry $b_{ij}^{(N)}$ is implicitly defined in (4.2). Given that successful decoding is only possible when a codeword is sent, we can write the throughput for

the adaptive system as

$$\sum_{i\in\mathcal{C}^\dagger}\sum_{j\in\mathcal{C}} P_{\mathrm{ds}}(c_j;c_i)\tilde{p}_C(c_i),$$

where $\tilde{p}_C(\cdot)$ is the invariant distribution associated with probability transition matrix $\tilde{\mathbf{B}}^{(N)}$.

When the average arrival rate is strictly less than the expected service rate, Foster's criteria guarantees that the corresponding Markov chain is positive recurrent [35, p. 167]. It is important to point out that channel memory and channel quality can greatly influence the expected service rate of a communication system. This is illustrated through numerical examples in the next chapter.

The channel state and the queue length at the onset of a codeword cycle, $Y_s = (C_{sN+1}, Q_s)$, jointly form a stochastic process with a countably infinite state space. A natural ordering for its elements is the following,

$$(c_1,0),\ldots,(c_k,0)(c_1,1),\ldots,(c_k,1)(c_1,2),\ldots$$

Collectively, the subset of states

$$\{(c_1,q),\ldots,(c_k,q)\}$$

is known as the qth level of the chain. Using this ordering and the level abstraction, we introduce a probability transition operator $\mathbf{T}$ for aggregate chain $\{Y_s\}$,

$$\mathbf{T} = \begin{pmatrix} \mathbf{C}_1 & \mathbf{C}_2 & \mathbf{0} & \mathbf{0} & \cdots \\ \mathbf{A}_0 & \mathbf{A}_1 & \mathbf{A}_2 & \mathbf{0} & \cdots \\ \mathbf{0} & \mathbf{A}_0 & \mathbf{A}_1 & \mathbf{A}_2 & \cdots \\ \mathbf{0} & \mathbf{0} & \mathbf{A}_0 & \mathbf{A}_1 & \cdots \\ \vdots & \vdots & \vdots & \vdots & \ddots \end{pmatrix}. \tag{4.4}$$

For the fixed antenna configuration case, the submatrices $\mathbf{A}_0, \mathbf{A}_1, \mathbf{A}_2$ are given by

$$\mathbf{A}_0 = \begin{bmatrix} \mu_{11} & \cdots & \mu_{1k} \\ \vdots & \ddots & \vdots \\ \mu_{k1} & \cdots & \mu_{kk} \end{bmatrix} \qquad \mathbf{A}_1 = \begin{bmatrix} \kappa_{11} & \cdots & \kappa_{1k} \\ \vdots & \ddots & \vdots \\ \kappa_{k1} & \cdots & \kappa_{kk} \end{bmatrix}$$

$$\mathbf{A}_2 = \begin{bmatrix} \lambda_{11} & \cdots & \lambda_{1k} \\ \vdots & \ddots & \vdots \\ \lambda_{k1} & \cdots & \lambda_{kk} \end{bmatrix}.$$

When the queue is empty, the block transitions are governed by

$$\mathbf{C}_1 = \begin{bmatrix} \kappa^0_{11} & \cdots & \kappa^0_{1k} \\ \vdots & \ddots & \vdots \\ \kappa^0_{k1} & \cdots & \kappa^0_{kk} \end{bmatrix} \qquad \mathbf{C}_2 = \begin{bmatrix} \lambda^0_{11} & \cdots & \lambda^0_{1k} \\ \vdots & \ddots & \vdots \\ \lambda^0_{k1} & \cdots & \lambda^0_{kk} \end{bmatrix}.$$

Similar definitions apply for systems with reconfigurable antennas; the appropriate entries are simply replaced by their homologs,

$$\tilde{\mu}_{ij}, \tilde{\kappa}_{ij}, \tilde{\lambda}_{ij}, \tilde{\kappa}^0_{ij} \text{ and } \tilde{\lambda}^0_{ij}.$$

In both cases, with and without adaptation, the corresponding Markov chains belong to the class of random processes with repetitive structures [25]. One can find the stationary distribution associated with $\mathbf{T}$ by inspecting the substochastic matrix $\mathbf{U}$ whose entry u_{ij} denotes the probability that, starting from state $(1, c_i)$, the Markov chain Y_s first re-enters level one through $(1, c_j)$ and does so without visiting any state at level zero. A probabilistic path-counting argument leads to Proposition .1.

Proposition .1 *Define* $\mathbf{U}_1 = \mathbf{A}_1$. *The iterative expression*

$$\mathbf{U}_{m+1} = \mathbf{A}_1 + \mathbf{A}_2 \left(\mathbf{I} - \mathbf{U}_m\right)^{-1} \mathbf{A}_0$$

is well-defined for all $m \in \mathbb{N}$*; its limit exists and*

$$\lim_{m\to\infty} \mathbf{U}_m = \mathbf{U}.$$

Let π represent the invariant distribution of the augmented Markov chain, and denote the subcomponents associated with level q by π_q,

$$\pi_q = \left(\Pr(Y = (c_1, q)), \ldots, \Pr(Y = (c_k, q))\right).$$

Proposition .2 *Define* $\mathbf{R} = \mathbf{A}_2(\mathbf{I} - \mathbf{U})^{-1}$ *and recall that the entries of* π *are non-negative and sum up to one. The invariant distribution induced by* $\mathbf{T}$ *is entirely determined through the following relations,*

$$\begin{bmatrix} \pi_0 & \pi_1 \end{bmatrix} \begin{bmatrix} \mathbf{C}_1 & \mathbf{C}_2 \\ \mathbf{A}_0 & \mathbf{A}_1 + \mathbf{R}\mathbf{A}_0 \end{bmatrix} = \begin{bmatrix} \pi_0 & \pi_1 \end{bmatrix} \tag{4.5}$$

and $\pi_q = \pi_1 \mathbf{R}^{q-1}$ *for* $q \geq 1$.

Propositions .1 & .2 provide an algorithmic blueprint to compute the stationary distribution of the augmented Markov chain: obtain $\mathbf{U}$ through repeated iterations; compute $\mathbf{R}$ and form irreducible and aperiodic probability transition matrix

$$\begin{bmatrix} \mathbf{C}_1 & \mathbf{C}_2 \\ \mathbf{A}_0 & \mathbf{A}_1 + \mathbf{R}\mathbf{A}_0 \end{bmatrix};$$

find its invariant distribution; append missing values of π using $\pi_q = \pi_1 \mathbf{R}^{q-1}$ and normalize.

Once the stationary distribution is acquired, we can compute several performance criteria of interest. We examine the average delay, the probability that the queue length exceeds a certain threshold and the decay rate of the queue occupancy. First,

we note that the expected queue length is given by

$$\sum_{q=0}^{\infty} q\pi_q \cdot \mathbf{1} = \pi_1 \left(\sum_{q=1}^{\infty} q\mathbf{R}^{q-1} \right) \cdot \mathbf{1}, \tag{4.6}$$

where $\mathbf{1}$ is a column vector of all ones. Using Little's formula, we deduce that the mean waiting time in the queue is simply (4.6) divided by expected arrival rate γ. The decay rate of the queue occupancy can be written as

$$\lim_{\tau \to \infty} \frac{1}{\tau} \log \Pr(Q \geq \tau) = \log \varrho(\mathbf{R}), \tag{4.7}$$

where $\varrho(\mathbf{R})$ is the spectral radius of $\mathbf{R}$; and its complementary cumulative distribution function is determined by the finite sum

$$\Pr(Q > \tau) = 1 - \sum_{q=0}^{\lfloor \tau \rfloor} \pi_q \cdot \mathbf{1}.$$

Next, we will use these performance criteria to show that time-dependencies in the underlying physical channel can adversely affect the behavior of a queued system. Moreover, having the ability to reconfigure an antenna structure at appropriate moments can help mitigate the undesirable effects of channel memory.

CHAPTER V

NUMERICAL RESULTS, SIMULATION, DISCUSSION AND CONCLUSIONS

A. Numerical Analysis and Results

We emphasis that the methodology introduced earlier applies to general finite-state erasure channels with memory, yet our numerical study focuses on the Gilbert-Elliott model depicted in Fig. 3. This model has received a fair amount of attention in the literature. It captures many of the features associated with wireless environments such as uncertainty, fading and channel memory. Still, this class of channels remains mathematically manageable due to its relative simplicity. Overall, the Gilbert-Elliott model provides valuable insights about the operation of wireless communication systems without being overly intricate, which gives ground for its adoption. This is especially relevant for a first characterization of the potential benefits associated with reconfigurable antenna structures.

1. Fixed vs. Reconfigurable Antenna Implementation

The choice of a hierarchical control policy for the Gilbert-Elliott channel with side information is straightforward. The only non-trivial candidate is the adaptive policy where the source triggers an antenna reconfiguration whenever the state of the channel is c_1 at the onset of a codeword transmission. The performance of this adaptive scheme is compared with the operation of a static system where the antenna structure is fixed and codewords are sent at every opportunity.

For the Gilbert-Elliott channel model, the stochastic matrix $\mathbf{B}$ reduces to

$$\mathbf{B} = \begin{bmatrix} b_{11} & b_{12} \\ b_{21} & b_{22} \end{bmatrix}$$

and has two degrees of freedom. One possible way to portray these degrees of freedom is to talk about the stationary probabilities of the states,

$$\Pr(C = c_1) = \frac{b_{21}}{b_{12} + b_{21}} \qquad \Pr(C = c_2) = \frac{b_{12}}{b_{12} + b_{21}},$$

and channel memory; this is the approach we use throughout. The memory of a Gilbert-Elliott channel can be expressed at the symbol level using $1 - b_{12} - b_{21}$. An equivalent way to characterize memory is to consider changes at the codeword level,

$$1 - b_{12}^{(N)} - b_{21}^{(N)} = (1 - b_{12} - b_{21})^N \in [0, 1). \tag{5.1}$$

It is typically more insightful to plot results using the latter scaling and, as such, this is the unit we employ in our figures. Additional system parameters are selected to approximate the operation of a GSM communication link. The block length is set to $N = 114$. New packets arrive at the source with probability $\gamma = 0.20$, and their expected length is $\rho^{-1} = 195$ bits. Based on a 4.615 ms codeword cycle, this yields a lightly loaded connection at roughly 8.45 kbps; these are realistic numbers for digital telephony.

We assess the performance of our competing systems when operating over erasure channels with an erasure probability equal to 20 percent. We first explore the impact of channel memory on overall performance. We study a channel model with $b_{12} = 4b_{21}$, $\varepsilon_1 = 0.5$ and $\varepsilon_2 = 0.125$. Channel correlation over time is varied progressively from the memoryless case to a very slow fading profile. Note that the value of K is throughput optimized for every parameter set and system implementation, leading to a fair comparison between schemes.

Fig. 6 displays maximum throughput in bits per channel use as a function of the memory coefficient defined in (5.1).

When channel memory is small, the communication system with a fixed antenna

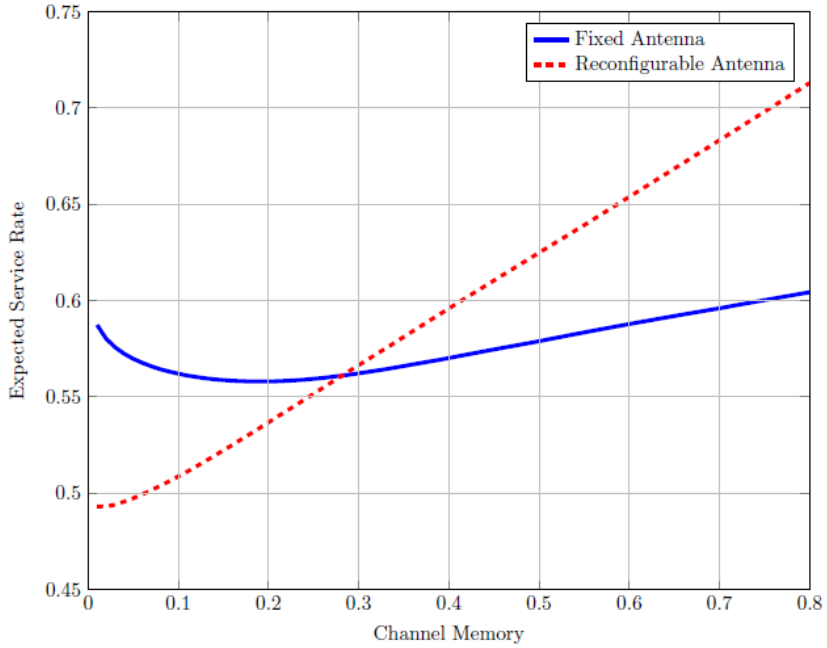

Fig. 6. The throughput of a traditional communication system is compared to that of a competing implementation with a reconfigurable antenna. As channel memory increases, the performance of the reconfigurable system surpasses the maximum service rate of the traditional implementation.

structure performs better. In particular, if the mixing time of the Gilbert-Elliott channel is shorter than a codeword transmission cycle, then reconfiguration offers little rewards. It is therefore more profitable to send codewords constantly. On the other hand, as the memory coefficient approaches one, the channel can get stuck in a bad fade for a prolonged period of time. This phenomenon almost certainly guarantees decoding failure at the next attempt; hence, it encourages the RF front-end to trigger a reconfiguration and seek a more auspicious channel realization. The crossover point in Fig. 6 is approximately 0.28. Interestingly, at this crossover point,

the expected sojourn time in state c_1 is approximately 113 bits, which is $1/b_{12}$, which is very close to the actual block length.

Similar curves can be generated for other parameter sets. Each of these curves identifies a crossover point in terms of channel memory and erasure probability where the throughput of the adaptive system overtakes the expected service rate of the traditional implementation. Plotting these points delineates the boundary of two regions, one where a static system with a fixed antenna structure performs better and a second region where the reconfigurable implementation delivers enhanced performance. This is illustrated in Fig. 7.

We can immediately see from this figure that channel correlation over time favors reconfigurable antenna systems. Also, experiencing vastly different channel qualities over the various fade levels benefits adaptive systems. Altogether, the capabilities of reconfigurable antennas seem better suited to harsh wireless environments.

We supplement the preceding results by investigating the performance of the two competing systems in relation to mean waiting time. This latter criterion is appropriate for lightly loaded connections and delay-sensitive applications such as mobile telephony and video conferencing. Again, we maintain the average rate of bit erasure at 20 percent, and we set the conditional probabilities of erasure to $\varepsilon_1 = 0.5$ and $\varepsilon_2 = 0.125$. As before, we vary the channel memory coefficient to first produce a memoryless process followed by increasingly correlated erasure sequences. Fig. 8 plots the mean waiting time at the source as a function of memory.

The crossover point where the switching system with a reconfigurable antenna structure overtakes the static implementation is approximately the same as in the case of throughput. In fact, preliminary results indicate that similar behavior can be observed for various parameter sets and different optimization criteria including mean waiting time, asymptotic decay rate in queue occupancy and threshold violation

probability, Fig. 9 shows our results for the threshold violation probability.

This robustness may be attributable to the simplicity of the Gilbert-Elliott model and may not hold for more complex channel models. This warrants further research, but lies outside the scope of this article. In practice, this suggests that good performance can be achieved with RF-agile antenna structures by identifying regions where reconfiguration should take place. The system can then estimate the current state of the channel and decide, according to its local map, whether or not a reconfiguration event should be triggered.

2. Fixed with Side Information

For fair comparison between a fixed antenna and a reconfigurable antenna that utilizes channel state information, we provide a simple study of the queueing behavior of a fixed antenna implementation that is provided with channel state information. For Such a system we assume that channel state information is available at the transmitter on the onset of a codeword, hence the transmitter can adaptively optimize performance by changing the code rate. We will consider the throughput metric, referring back to the equation of throughput,

$$\sum_{j} P_{\mathrm{ds}}(C_j, C_i)$$

This equation implicitly depends on the code rate. If the channel is good the transmitter can adaptively use a higher code rate, and visa versa. We thus denote the code rate as a function of the channel state and we use the notation $K(C_i)$. The probability of decoding failure is expressed as follows

$$\sum_{e=0}^{N} P_{\mathrm{f}}(N - K(C_i), e) \Pr\left(E = e, C_{N+1} = C_j | C_i = C_1\right).$$

We next examine throughput in bits per channel use, for a two channel realization, as in the Gilbert-Elliott case, using above notation and assumptions

$$K^*(C_1) = \underset{K(C_1)}{\operatorname{argmax}} K(C_1) \sum_j \sum_e (1 - P_{\mathrm{f}}(N - K(C_1), e)) \Pr\left(E = e, C_{N+1} = C_j | C_i = C_1\right)$$

$$K^*(C_2) = \underset{K(C_2)}{\operatorname{argmax}} K(C_2) \sum_j \sum_e (1 - P_{\mathrm{f}}(N - K(C_2), e)) \Pr\left(E = e, C_{N+1} = C_j | C_i = C_2\right)$$

Then throughput for fixed antenna system with channel state information side information can be expressed as

$$p_C(C_1).K^*(C_1) + p_C(C_2).K^*(C_2)$$

Fig. 10 shows throughput of three systems, traditional fixed antenna, traditional fixed antenna with side channel sate information at the transmitter, and reconfigurable antenna. As shown in the figure, the performance of the traditional system with side channel state information naturally shows better performance than the traditional system that is not powered by the side information. Still the reconfigurable antenna shows enhanced performance in the high memory region. And that expected as the reconfigurable antenna system posses more degrees of freedom.

Next we explore the change in crossover region, between the traditional and reconfigurable antenna, and the traditional and fixed with side channel state information. Fig. 11 shows the region boundaries for the two crossover regions. From the figure, it can be concluded that a reconfigurable antenna implementation delivers better throughput over a wider range of system parameters; high channel memory values and erasure probabilities.

3. n-State Channel Simulation

As our work builds on the realization of the wireless communication channel as a finite-state Markov Model, we attempt to simulate some of the above results. As we have already summarized in second chapter, finite-state channel models can be constructed from statistical fading models such as the Clark's model for Rayleigh fading channels. The equations to derive the finite-state Markov model parameters from the Rayleigh model have been derived by Wang and Moayeri [29].

The Signal-to-Noise range is partitioned into equiprobable regions, then given system parameters such as the Doppler shift and transmission rate, the probability transition matrix and the error probabilities associated with the each state discrete memoryless channel are calculated.

We design our Monte Carlo simulation for the threshold violation probability performance metric, and first we explore the behavior of the finite-state channel model under this metric for different number of states. Here the threshold value is set to $\tau = 12$, fading model doppler shift is varied over the range $[1, 100](Hz)$, and transmission rate is set at 1000. Queueing parameters are set as, arrival rate $\gamma = 0.2$, $N = 114$, $\rho = 1/L$ and $L = 1000$. Fig. 12 shows the simulations results for number of finite states of the channel $2, 3, 4, 5, 6, 7, 8, 16$, from which we notice that as number of states increased we obtain a more rich realization of the performance plot, which exhibits that when in a deep fade at high channel memory, corresponding to low Doppler shifts, is likely to stay in deep fade.

B. Conclusions

This preliminary study offers supporting evidence to the claim that reconfigurable antenna structures can improve the performance of communication systems signifi-

cantly. For the reconfiguration process to be beneficial, the potential rewards of a reconfiguration event must offset the costs of a loss of codeword transmission opportunity. Two conditions appear to influence this balance. The coherence time of the physical channel must be on the order of the codeword cycle or longer. Furthermore, the quality of the channel must vary significantly over the different fade levels. Slow fading channels appear to be great prospects for reconfigurable antenna systems with adaptive control policies.

Future studies should address practical issues such as channel estimation and decision rule based on limited information. Once side information becomes available at the transmitter, rate adaptation and power control can be employed in conjunction with reconfigurable antenna structures. Extending the queueing formulation to account for these techniques is an interesting goal. Also, the postulate that virtual channels are independent from one another should be explored through empirical measurements. A strong positive correlation among virtual channels would reduce the expected returns of a reconfiguration event. These are promising avenues of future research that may broaden the application potential of reconfigurable antennas and help improve the performance of wireless communication systems.

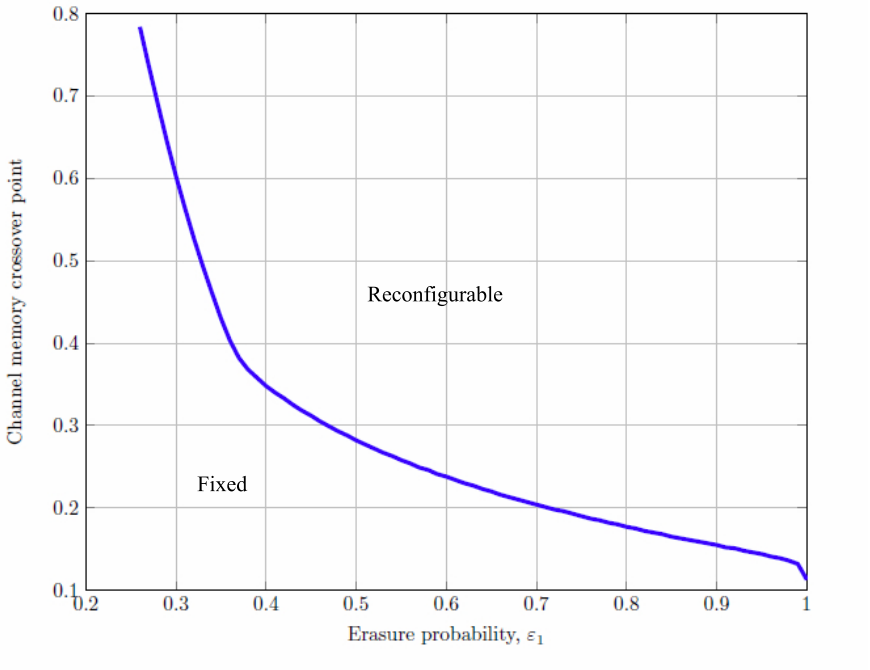

Fig. 7. System parameters determine which implementation delivers better throughput, the static system with a fixed antenna structure (Static) or the switching scheme with reconfigurable antennas (Switch). Correlation and fade differentiation are advantageous to the RF-agile switching scheme. In this figure, the probability of erasure is set at 0.20 and $\varepsilon_2 = (1 - \varepsilon_1)/4$.

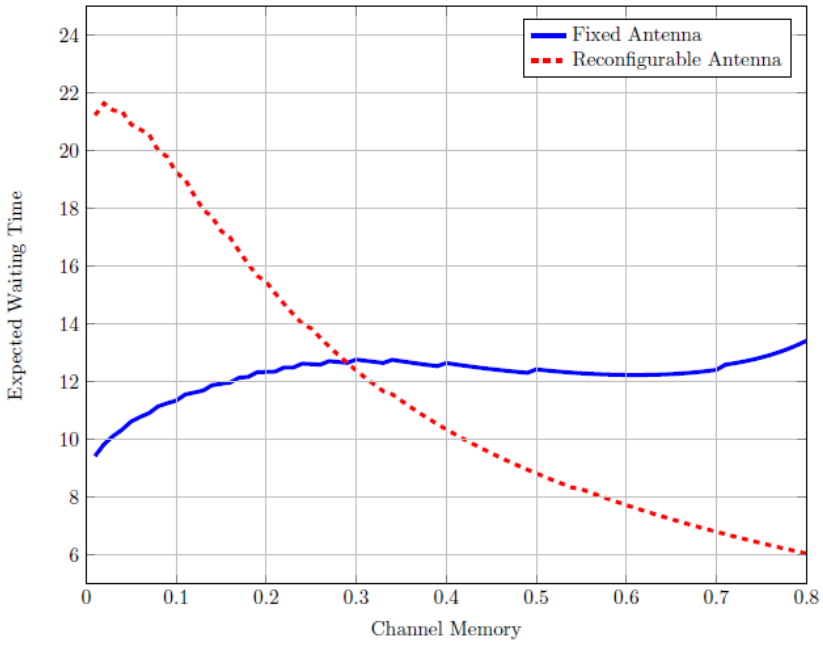

Fig. 8. Mean waiting times for traditional and switching systems are plotted as functions of channel memory; a smaller waiting time is desirable. When the channel is weakly correlated over time, the system with a fixed antenna configuration performs better. On the other hand, in slow fading scenarios, the adaptive implementation with a reconfigurable antenna structure becomes advantageous.

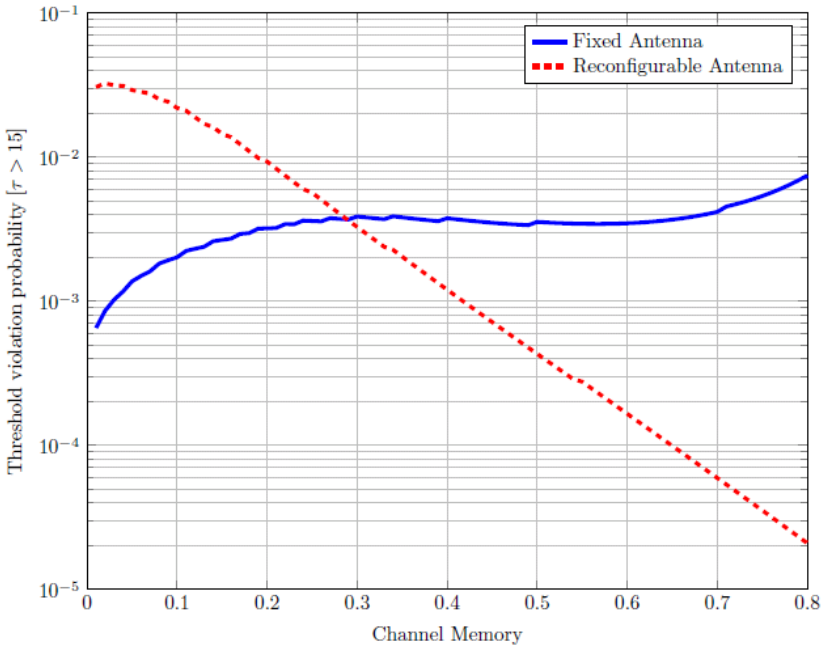

Fig. 9. Threshold violation probability of a traditional communication system is compared to that of a competing implementation with a reconfigurable antenna. We seek a lower threshold violation probability. As channel memory increases, the performance of adaptive systems with reconfigurable system surpasses that of the traditional systems.

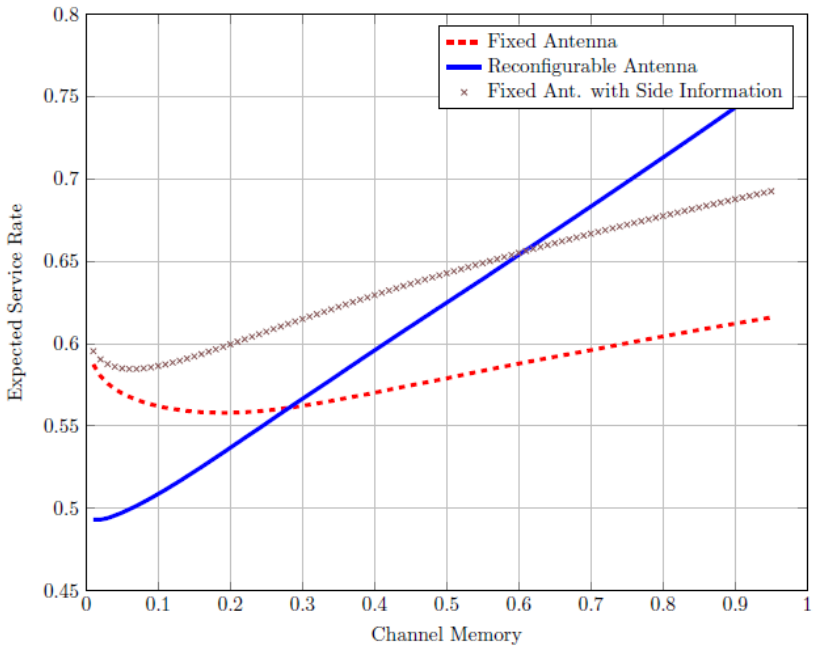

Fig. 10. The throughput of a traditional communication system that is provided with side information about channel state is compared to that of a competing implementation with a reconfigurable antenna and to a traditional system without the side information, As channel memory increases, the performance of the reconfigurable system surpasses the maximum service rate of the traditional implementation with side channel state information.

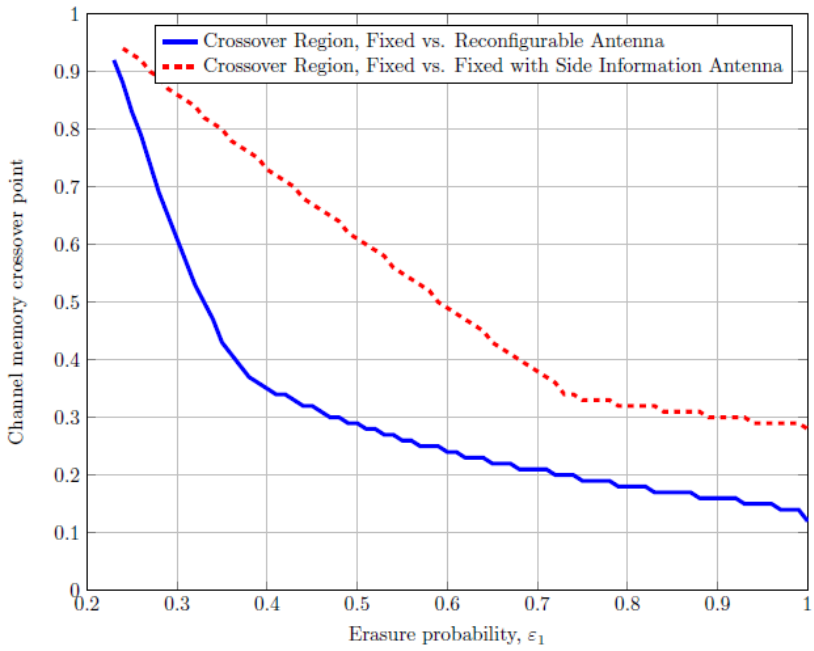

Fig. 11. We employ system parameters to study the change in crossover boundary region, for both the reconfigurable antenna and traditional fixed antenna with side channel state information, each plot illustrate the crossover boundary for the competing scheme with the traditional fixed antenna implementation. Correlation and fade differentiation are advantageous to the RF-agile switching scheme. In this figure, the probability of erasure is set at 0.20 and $\varepsilon_2 = (1 - \varepsilon_1)/4$.

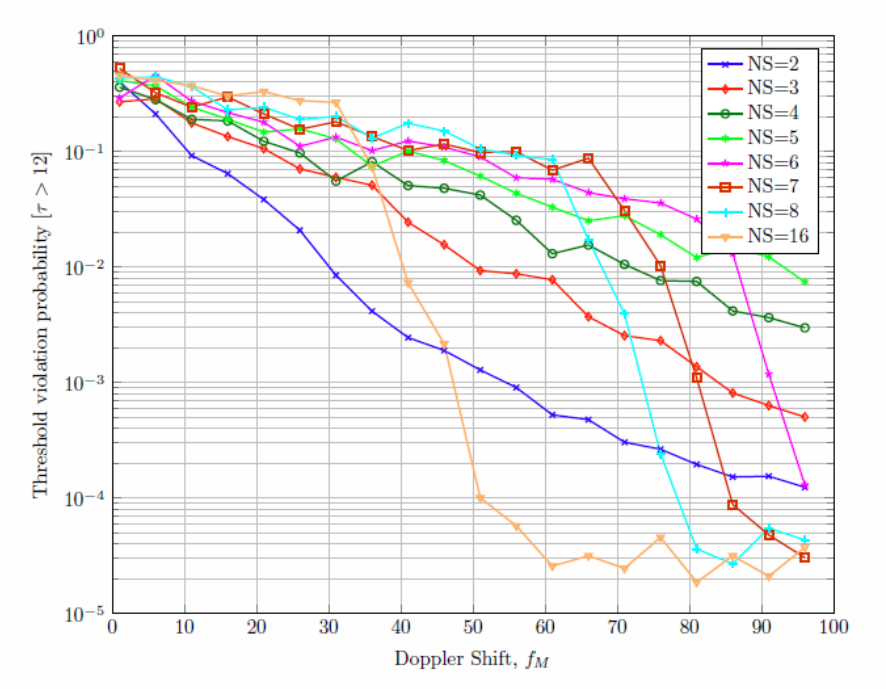

Fig. 12. A Finite-State Markov model is constructed based on a Rayleigh fading model, as the number of states in the Markov model is increased, we gain a more rich realization of the channel that is more descriptive. Figure shows Monte Carlo simulation results for threshold violation probability performance metric, for number of states $NS \in 2, 3, 4, 5, 6, 7, 8, 16$.

REFERENCES

[1] T. S. Rappaport, *Wireless Communications: Principles and Practice*, 2nd ed. Upper Saddle River, N.J.: Prentice Hall PTR, 2002.

[2] G. L. Stüber, *Principles of Mobile Communication*, 2nd ed. New York: Springer, 2000.

[3] L. Zheng and D. Tse, "Diversity and multiplexing: A fundamental tradeoff in multiple-antenna channels," *Information Theory, IEEE Transactions on*, vol. 49, no. 5, pp. 1073 – 1096, May 2003.

[4] G. J. F. Jr., "Layered space-time architecture for wireless communication in a fading environment when using multi-element antennas," *Bell Labs Technical Journal*, vol. 1, no. 2, p. 4159, 1996.

[5] R. Berry and R. Gallager, "Communication over fading channels with delay constraints," *IEEE Transactions on Information Theory*, vol. 48, no. 5, pp. 1135–1149, May 2002.

[6] A. Laourine and L. Tong, "Betting on Gilbert-Elliot channels," *IEEE Transactions on Wireless Communications*, vol. 9, no. 2, pp. 723–733, 2010.

[7] G. H. Huff, J. Feng, S. Zhang, G. Cung, and J. T. Bernhard, "Directional reconfigurable antennas on laptop computers: Simulation, measurement and evaluation of candidate integration positions," *IEEE Transactions on Antennas and Propagation*, vol. 52, no. 12, pp. 3220–3227, 2004.

[8] T. L. Roach, G. H. Huff, and J. T. Bernhard, "A comparative study of diversity gain and spatial coverage: Fixed versus reconfigurable antennas for portable

devices," *Microwave and Optical Technology Letters*, vol. 49, no. 3, pp. 535–539, 2007.

[9] S. Yang, C. Zhang, H. Pan, A. Fathy, and V. Nair, "Frequency-reconfigurable antennas for multiradio wireless platforms," *IEEE Microwave Magazine*, vol. 10, no. 1, pp. 66–83, 2009.

[10] H. Rajagopalan, Y. Rahmat-Samii, and W. A. Imbriale, "RF MEMS actuated reconfigurable reflectarray patch-slot element," *IEEE Transactions on Antennas and Propagation*, vol. 56, no. 12, pp. 3689–3699, 2008.

[11] G. H. Huff, D. L. Rolando, P. Walters, and J. McDonald, "A frequency reconfigurable dielectric resonator antenna using colloidal dispersions," *IEEE Antennas and Wireless Propagation Letters*, vol. 9, pp. 288–290, 2010.

[12] C. J. Panagamuwa, A. Chauraya, and J. C. Vardaxoglou, "Frequency and beam reconfigurable antenna using photoconducting switches," *IEEE Transactions on Antennas and Propagation*, vol. 54, no. 2, pp. 449–454, 2006.

[13] D. Piazza, N. J. Kirsch, A. Forenza, R. W. Heath, and K. R. Dandekar, "Design and evaluation of a reconfigurable antenna array for MIMO systems," *IEEE Transactions on Antennas and Propagation*, vol. 56, no. 3, pp. 869–881, 2008.

[14] A. Mahanfar, C. Menon, and R. G. Vaughan, "Smart antennas using electroactive polymers for deformable parasitic elements," *Electronics Letters*, vol. 44, no. 19, pp. 1113–1114, 2008.

[15] M. P. Daly and J. T. Bernhard, "Beamsteering in pattern reconfigurable arrays using directional modulation," *IEEE Transactions on Antennas and Propagation*, vol. 58, no. 7, pp. 2259–2265, 2010.

[16] A. F. Molisch and M. Z. Win, "Mimo systems with antenna selection," *IEEE Microwave Magazine*, vol. 5, no. 1, pp. 46–56, 2004.

[17] T. Gou, C. Wang, and S. A. Jafar, "Aiming perfectly in the dark – blind interference alignment through staggered antenna switching," *IEEE Transactions on Signal Processing*, vol. 59, no. 6, pp. 2734–2744, 2011.

[18] J. G. Kim and M. M. Krunz, "Bandwidth allocation in wireless networks with guaranteed packet-loss performance," *IEEE/ACM Transactions on Networking*, vol. 8, no. 3, pp. 337–349, June 2000.

[19] D. Wu and R. Negi, "Effective capacity: A wireless link model for support of quality of service," *IEEE Transactions on Wireless Communications*, vol. 2, no. 4, pp. 630–643, 2003.

[20] L. Liu, P. Parag, J. Tang, W.-Y. Chen, and J.-F. Chamberland, "Resource allocation and quality of service evaluation for wireless communication systems using fluid models," *IEEE Transactions on Information Theory*, vol. 53, no. 5, pp. 1767–1777, May 2007.

[21] P. Parag, J.-F. Chamberland, H. D. Pfister, and K. R. Narayanan, "On the queueing behavior of random codes over a Gilbert-Elliott erasure channel," in *2010 IEEE International Symposium on Information Theory Proceedings (ISIT)*. IEEE, 2010, pp. 1798–1802.

[22] E. N. Gilbert, "Capacity of a burst-noise channel," *Bell Syst. Tech. J*, vol. 39, no. 5, pp. 1253–1265, 1960.

[23] E. O. Elliott, "Estimates of error rates for codes on burst-noise channels," *Bell Syst. Tech. J*, vol. 42, no. 5, pp. 1977–1997, 1963.

[24] M. F. Neuts, *Structured stochastic matrices of M/G/1 type and their applications*. New York: Marcel Dekker, 1989.

[25] ——, *Matrix-Geometric Solutions in Stochastic Models: An Algorithmic Approach*. Baltimore, MD. : Johns Hopkins University Press, 1981.

[26] B. Hajek, "Birth-and-death processes on the integers with phases and general boundaries," *Journal of Applied Probability*, vol. 19, no. 3, pp. 488–499, 1982.

[27] A. Goldsmith, *Wireless Communications*. New York: Cambridge University Press, 2005.

[28] C. E. Shannon, "Certain results in coding theory for noisy channels," *Information and Control*, vol. 1, no. 1, pp. 6 – 25, 1957. [Online]. Available: http://www.sciencedirect.com/science/article/pii/S0019995857900396

[29] H. S. Wang and N. Moayeri, "Finite state Markov channel – A useful model for radio communication channels," *IEEE Transactions on Vehicular Technology*, vol. 44, no. 1, pp. 163–171, February 1995.

[30] M. M. Krunz and J. G. Kim, "Fluid analysis of delay and packet discard performance for QoS support in wireless networks," *IEEE Journal on Selected Areas in Communications*, vol. 19, no. 2, pp. 384–395, 2001.

[31] P. Sadeghi, R. A. Kennedy, P. Rapajic, and R. Shams, "Finite-state Markov modeling of fading channels: A survey of principles and applications," *IEEE Signal Processing Magazine*, vol. 25, no. 5, pp. 57–80, September 2008.

[32] L. Wilhelmsson and L. B. Milstein, "On the effect of imperfect interleaving for the Gilbert-Elliott channel," *IEEE Transactions on Communications*, vol. 47, no. 5, pp. 681–688, May 1999.

[33] J.-F. Chamberland, H. Pfister, and S. Shakkottai, "First-passage time analysis for digital communication over erasure channels with delay-sensitive traffic," in *2010 48th Annual Allerton Conference on Communication, Control, and Computing (Allerton)*. IEEE, 2010, pp. 399–405.

[34] T. Richardson and R. Urbanke, *Modern Coding Theory*. New York: Cambridge University Press, 2008.

[35] P. Brémaud, *Markov Chains: Gibbs Fields, Monte Carlo Simulation, and Queues*, ser. Texts in Applied Mathematics. New York: Springer Verlag, 1999, vol. 31.

[36] J. R. Norris, *Markov Chains*, ser. Cambridge Series in Statistical and Probabilistic Mathematics. New York: Cambridge University Press, 1997.

VITA

Name: Eman Mahmoud Hammad

Address: Eman Mahmoud Hammad,
C/O Jean-Francois Chamberland,
Department of Electrical and Computer Engineering,
Texas A&M University,
214 Zachry Engineering Center,
College Station, Texas 77843-3128

Email Address: eman.hammad@gmail.com

Education: B.S., Electrical Engineering, University of Jordan, 2000
M.S., Electrical Engineering, Texas A&M University, 2011

The typist for this thesis was Eman Mahmoud Hammad.